A Fourier Analysis of Earthquake Frequencies

Rajan Agarwal

Introduction

This paper introduces a novel approach for modeling the attenuation of earthquake frequencies with respect to distance from the epicenter. This geological and graphical analysis, utilizing the Fourier Transform, analyzes the temporal frequency spectrum of seismic waves recorded at various distances from the epicenter to accurately predict the decay of earthquake frequencies. This method represents a significant improvement over previously employed techniques, as it is theoretically grounded and offers a more precise prediction of earthquake frequency decay. Our method is validated using a comprehensive dataset and demonstrates practical utility in a variety of contexts. This work represents a significant advancement in earthquake seismology, creating new opportunities for cost-efficient 3D testing of architectural design in earthquake-prone areas.

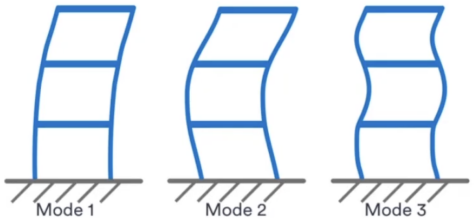

Figure 1: Sinusoidal Movement of Buildings in Earthquake Movement (Pekar, 2020)

Consider a building. Under standard conditions, its movement is defined by a Single Degree of Freedom (SDOF) as it can be modeled by one frequency. However, earthquake movements, similar to most signals, are an intricate series of waves that are superimposed on one another. These waves have Multiple Degrees of Freedom (MDOF), and can be broken down into a series of sinusoidal functions. These building movements and, by extension, earthquake movements, can be simplified to a series of modes that produce frequencies in complement to each other. Seismologists, who studied the 2015 Nepal earthquake, published strong ground motion data that represented continuous functions in the time domain.

These three-dimensional earthquake ground motion waves, collected at multiple points (KTP, TVU, PTN, THM) with respect to longitude, latitude and elevation (NS, EW, UD), are in the time

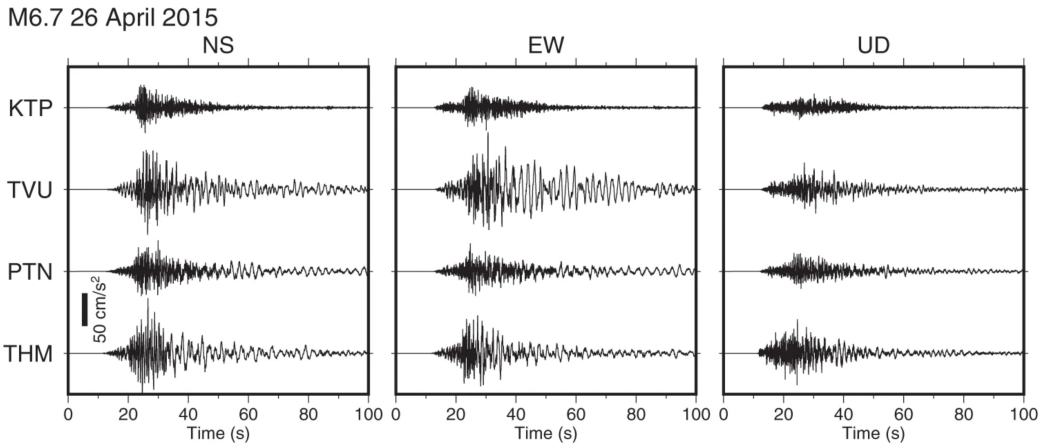

Figure 2: Sample strong ground motion data of the 2015 Nepal Earthquake (Shigefuji et al., 2022)

domain. This data, however, is fairly abstract and does not immediately provide the necessary information to find frequencies. This is where the Fourier series is important, a mathematical concept that defines each wave as a signal that can be represented as the sum of harmonic sinusoidal functions; in this way, asymmetrical—and often convoluted—waves produced by earthquakes (Figure 2) can be approximated as a sum of cosine (even) and sine (odd) functions. There are multiple interpretations of a Fourier series, one of which that represents these sine and cosine functions as points on a complex plane. With this complex interpretation, frequencies can be determined by decomposing these functions into their **real** and **imaginary** components on an Argand plane.

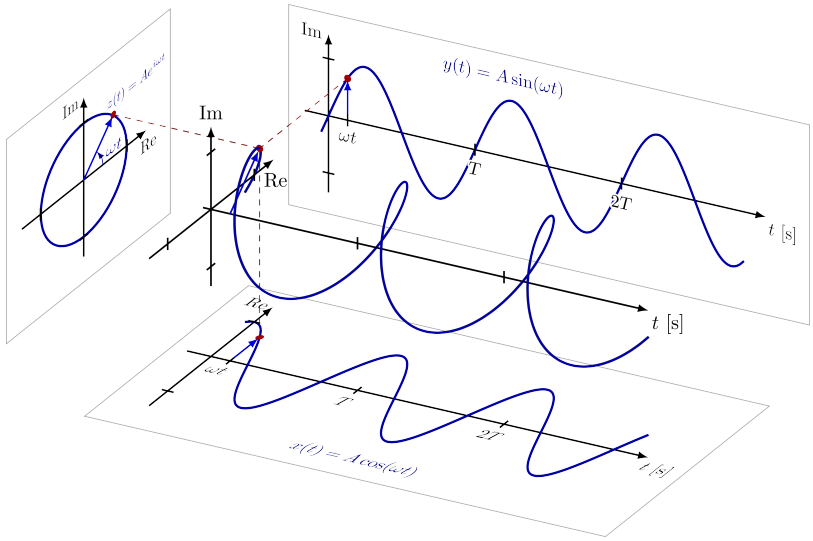

Figure 3: Complex interpretation of the Fourier Series (Aldeen, 2020)

The Fourier Transform

Calculating the frequencies of a continuous function first requires an understanding of how the individual building blocks, sine and cosine components, interact. Consider the sum as follows.

$$\sum_{n=0}^{\infty} \alpha_n cos(nt) + \sum_{n=0}^{\infty} \beta_n sin(mx)$$

Here, the Fourier coefficients are defined as:

$$\alpha_n = \frac{1}{\pi} \int_{-\pi}^{\pi} f(t) cos(nt) dx, n = 0, 1, ...,$$

$$\beta_n = \frac{1}{\pi} \int_{-\pi}^{\pi} f(t) sin(mt) dx, m = 0, 1, ...,$$

By *Euler's Theorem* and *deMoivre's Theorem*, the *sine* and *cosine* values from each can be represented as complex numbers. Now, e^{it} can be simplified to isolate for $sin(t)$ and $cos(t)$.

$$e^{it} = cos(t) + isin(t)$$

$$e^{-it} = cos(-t) + isin(-t)$$

$$e^{it} - e^{-it} = 2isin(t), sin(t) = \frac{e^{it} - e^{-it}}{2i}$$

$$e^{it} + e^{-it} = 2cos(t), cos(t) = \frac{e^{it} + e^{-it}}{2}$$

Let C represent the complex coefficient, where $C = \alpha_n + i\beta_n$ and its conjugate is $C^* = \alpha_n - i\beta_n$ at $-2\pi t$. By interpreting the sum in the complex plane,

$$f(t) = \sum_{n=1}^{\infty} \left[\alpha_n (\frac{e^{-2\pi int} + e^{2\pi int}}{2}) + \beta_n (\frac{e^{-2\pi int} - e^{2\pi int}}{2i}) \right]$$

Given our complex numbers, these equations can be simplified into a sum on the complex plane.

$$f(t) = \sum_{n=1}^{\infty} (\frac{\alpha_n - i\beta_n}{2}) e^{-2\pi int} + \sum_{n=1}^{\infty} (\frac{\alpha_n + i\beta_n}{2}) e^{2\pi int}$$

$$f(t) = \sum_{n=1}^{\infty} C^*{}_n \, e^{-2\pi int} + \sum_{n=1}^{\infty} C_n e^{2\pi int}$$

By complex properties, since $C_n = C^*{}_{-n}$ and $C^*{}_n \, e^{-2\pi int} = C^*{}_{-n} \, e^{2\pi int}$, the equation becomes:

$$f(t) = \sum_{n=1}^{-\infty} C^*{}_{-n} \, e^{2\pi int} + \sum_{n=1}^{\infty} C_n e^{2\pi int} = \sum_{n=-\infty}^{\infty} C_n e^{2\pi int} \tag{1}$$

This sum represents both the imaginary and real components of a continuous function. Despite this effectively modeling seismic readings in their components, a function is required to transform a signal between domains. Therefore, this sum should act as a filtering mechanism to transform a function $f(t)$ between the time and frequency domain.

The coefficient, C_n, may be expanded in a similar way.

$$C_n = (\alpha_n + i\beta_n)$$

$$C_n = \left[\int_0^1 f(t) cos(nt) dt + i \int_0^1 f(t) sin(nt) dt \right]$$

$$C_n = \left[\int_0^1 f(t) \frac{e^{int} + e^{-int}}{2} dt + \int_0^1 f(t) \frac{e^{int} - e^{-int}}{2i} dt \right]$$

$$C_n = \int_0^1 f(t) e^{int} dt$$

Using *deMoivre's theorem*, the Fourier Transform can be simplified for $-2\pi t$.

$$C_n = \int_0^1 f(t) e^{-2\pi int} dt \tag{2}$$

With these two equations, a continuous function in the time domain can be transformed into a discrete function in the frequency domain. This is what we call a Fourier Transform, which can be applied to the intricate signal processing of seismic waves in earthquakes and can then be **filtered** into separate frequency distributions.

Applying the Fourier Transform

While a lot of data on earthquakes are public, the majority of waveforms are raw data files that are not open-sourced. This served as a challenge in the investigation, as I could no longer explore the initial earthquake of investigation. This required a new focus to create a universal formula for earthquake decay, understanding how frequencies act and how buildings can be optimized around them. For one earthquake, in the Indian Ocean in 2012, the raw data appears as follows with three readings (X, Y, Z) at each set of coordinates, a certain distance from the epicenter.

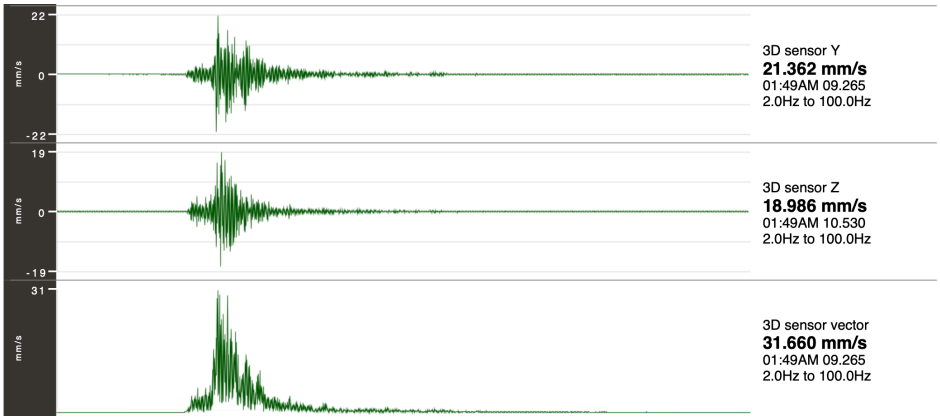

Figure 4: Raw Data from 2012 Earthquake in the Indian Ocean

Using the aforementioned Fourier Transform in the complex plane, this continuous series can be analyzed in the context of a frequency domain. The filtering function requires technology, but can be estimated by applying the Fourier Transform to an estimated function, as a dampened sine wave: $f(t) = 50e^{-0.2t}sin(t)$.

Seismic signals are broken down into p and s waves, known as primary and secondary waves

respectively. Here, p waves, or compression waves, are a type of seismic wave that travel through the Earth's interior. They are characterized by their ability to compress and expand materials through which they pass, and are responsible for the initial shaking that is often felt during an earthquake. In contrast, s waves are a type of seismic wave that are slower and less energetic than p waves. They are characterized by their ability to shear or deform materials through which they pass, and typically cause more severe damage during an earthquake (Manoa, 2007).

Since both p and s waves can be modeled by the same equation, $50e^{-0.2t}sin(t)$, the filtering of this equation is effective. Initially, it is known that by the properties of the Discrete Fourier Transform, which was previously derived:

$$C_n = \int_0^1 f(t)e^{-2\pi int}dt$$

$$f(t) = \sum_{-\infty}^{\infty} C_n e^{2\pi int}$$

First, the Fourier expansion coefficient, C_n, must be determined for $f(t) = 50e^{-0.2t}sin(t)$. This dampened sine wave can be transformed to represent a sum of sinusoidal functions in the frequency domain. Thus,

$$C_n = \int_0^1 e^{-2\pi int}(50e^{-0.2t}sint)dt$$

By the principles of *deMoivre's Theorem*, we know that $sin(t) = \frac{e^{it}-e^{-it}}{2i}$:

$$C_n = \int_0^1 e^{-2\pi int}(50e^{-0.2t})(\frac{1}{2i}e^{it} - \frac{1}{2i}e^{-it}))dt$$

$$C_n = \int_0^1 \frac{25}{i}e^{-2\pi int}e^{-0.2t}(e^{it} - e^{-it})dt$$

By the property of the complex conjugate, $\frac{1}{i} = \frac{i}{-1} = -i$.

$$C_n = -25i\int_0^1 (e^{-2\pi int}e^{-0.2t}e^{it} - e^{-2\pi int}e^{-0.2t}e^{-it})dt$$

When distributing the integral, and combining the exponents using exponent law:

$$C_n = -25i\int_0^1 (e^{(-2\pi in-0.2+i)t} - e^{(-2\pi in-0.2-i)t})dt$$

$$C_n = -25i\left[\int_0^1 e^{(-2\pi in-0.2+i)t}dt\right]\left[\int_0^1 e^{(-2\pi in-0.2-i)t}dt\right]$$

Consider the integrals I_1 and I_2, such that:

$$I_1 = \int_0^1 e^{(-2\pi in-0.2+i)t}dt \tag{3}$$

$$I_2 = \int_0^1 e^{(-2\pi in-0.2-i)t}dt \tag{4}$$

For each, the integral should be relative to du instead of dt. I_1 and I_2 will be integrated by using substitution, hence it must be integrated with respect to u, a dummy variable, instead of t.

$$du = (-2\pi in - 0.2 + i)dt$$

Isolating for dt,

$$dt = \frac{1}{-2\pi in - 0.2 + i} du$$

Similarly, in I_2:

$$u = (-2\pi in - 0.2 - i)t$$

$$du = (-2\pi in - 0.2 - i)dt$$

$$dt = \frac{1}{-2\pi in - 0.2 - i} du$$

Hence, the initial function can be written relative to du, which exists in the frequency domain.

$$C_n = -25i \left[\frac{1}{-2\pi in - 0.2 + i} \int_0^1 e^u du \right] \left[\frac{1}{-2\pi in - 0.2 - i} \int_0^1 e^u du \right]$$

By evaluating the definite integral, it can be written as follows:

$$C_n = -25i \left[\frac{1}{-2\pi in - 0.2 + i} e^{(-2\pi in - 0.2 + i)t} \Big|_0^1 - \frac{1}{-2\pi in - 0.2 - i} e^{(-2\pi in - 0.2 - i)t} \Big|_0^1 \right]$$

$$C_n = \left[\frac{-25i}{-2\pi in - 0.2 + i} e^{(-2\pi in - 0.2 + i)t} + \frac{-25i}{-2\pi in - 0.2 - i} e^{(-2\pi in - 0.2 - i)t} \right]_0^1$$

Then, by properties of the Anti-derivative of our integral, it can be expanded to reflect the complex components:

$$C_n = \left(\frac{-25i}{-2\pi in - 0.2 + i} e^{-2\pi in - 0.2 + i} + \frac{25i}{-2\pi in - 0.2 - i} e^{-2\pi in - 0.2 - i} \right)$$

$$- \left(\frac{-25i}{-2\pi in - 0.2 + i} + \frac{25i}{-2\pi in - 0.2 - i} \right)$$

$$C_n = \frac{25i}{-2\pi in - 0.2 + i} \left(1 - e^{-2\pi in - 0.2 + i} \right) + \frac{25i}{-2\pi in - 0.2 - i} \left(e^{-2\pi in - 0.2 - i} - 1 \right)$$

To factor out an i from the numerator,

$$C_n = \frac{25i}{i(-2\pi n - \frac{0.2}{i} + 1)}\Big(1 - e^{-2\pi in - 0.2 + i}\Big) + \frac{25i}{i(-2\pi n - \frac{0.2}{i} - 1)}\Big(e^{-2\pi in - 0.2 - i} - 1\Big)$$

$$C_n = \frac{25}{-2\pi n - \frac{0.2}{i} + 1}\Big(1 - e^{-2\pi in - 0.2 + i}\Big) + \frac{25}{-2\pi n - \frac{0.2}{i} - 1}\Big(e^{-2\pi in - 0.2 - i} - 1\Big)$$

Thus, the coefficient for the Fourier Transform can be simplified. While it can be simplified further with a common denominator, the equation becomes unnecessarily repetitive. Therefore, the the C_n coefficient, as follows, is the most simplified version.

$$C_n = \frac{25}{-2\pi n + 0.2i + 1}\Big(1 - e^{-2\pi in - 0.2 + i}\Big) + \frac{25}{-2\pi n + 0.2i - 1}\Big(e^{-2\pi in - 0.2 - i} - 1\Big)$$

This equation represents the coefficient of the Discrete Fourier Expansion of our estimated function, the dampened sine wave $f(t) = 50e^{-0.2t}sin(t)$, transforming our continuous time domain into a discrete frequency domain.

Given this simplification, the coefficient can be implemented back into the initial function for $f(t)$, representing the sum of the waves as an expansion of frequencies.

$$f(t) = \sum_{-\infty}^{\infty} C_n e^{2\pi int}$$

$$f(t) = \sum_{-\infty}^{\infty} \Big[\frac{25}{-2\pi n + 0.2i + 1}\Big(1 - e^{-2\pi in - 0.2 + i}\Big) + \frac{25}{-2\pi n + 0.2i - 1}\Big(e^{-2\pi in - 0.2 - i} - 1\Big)\Big] e^{2\pi int}$$

By substitution to simplify the function, the Fourier Transform for our dampened sine wave can be simplified as follows:

$$f(t) = \sum_{-\infty}^{\infty} \Big[\frac{25e^{2\pi int}}{-2\pi n + 0.2i + 1}\Big(1 - e^{-2\pi in - 0.2 + i}\Big) + \frac{25e^{2\pi int}}{-2\pi n + 0.2i - 1}\Big(e^{-2\pi in - 0.2 - i} - 1\Big)\Big]$$

This equation proves the most fundamental principle of this investigation: **the frequency of**

seismic waves. This filtering function, for the continuous series of a seismic wave, can create a distribution of frequencies.

Frequency Distribution

Given the aggregate nature of a seismic wave, as well as the large scale of datasets, analyzing each frequency required technology. Here, I used the derived function to design an algorithm in Python and MATLAB that, with the Fourier Transform, converts waveforms into frequency distributions.

Consider a waveform input from all three dimensions, in Figure 4 for example. This graph plots frequency per unit time against particle velocity in units (mm/s). Unfortunately, as a continuous function, the computing power required to achieve a full Fourier Transform is unattainable. Instead of iterating through a continuous function, the derived equation was calculated at discrete points. Then, these points were plotted against particle velocity per unit frequency.

In Figure 5, three-dimensional seismic waves are discretely transformed. A simpler filtered distribution was created, that reduces a large amount of the noise. Then, once reconstructed, it plots the frequencies in each of the dimensions.

By using $f(t) = \frac{25e^{2\pi int}}{-2\pi n+0.2i+1}\left(1-e^{-2\pi in-0.2+i}\right)+\frac{25e^{2\pi int}}{-2\pi n+0.2i-1}\left(e^{-2\pi in-0.2-i}-1\right)$ to estimate discrete values, and then reconstructing a wave in the new domain using an existing filtering function, frequency distributions can be produced. In the case of Figure 4, for example, the distribution for the X, Y and Z axis produces Figure 6, further applied to all frequencies in the dataset.

Each of these frequencies are associated with a position based on latitude, longitude and elevation. While these values have independent properties, they form direction vectors when compared to a central epicenter. When given an initial point, it can be compared to the epicenter, given that

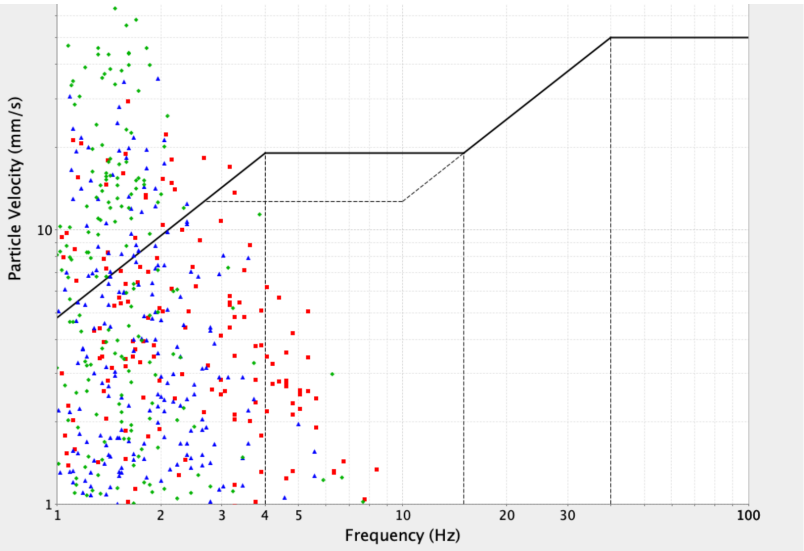

Figure 5: Discrete Particle Velocity Distribution per Frequency (Green = X, Blue = Y, Red = Z)

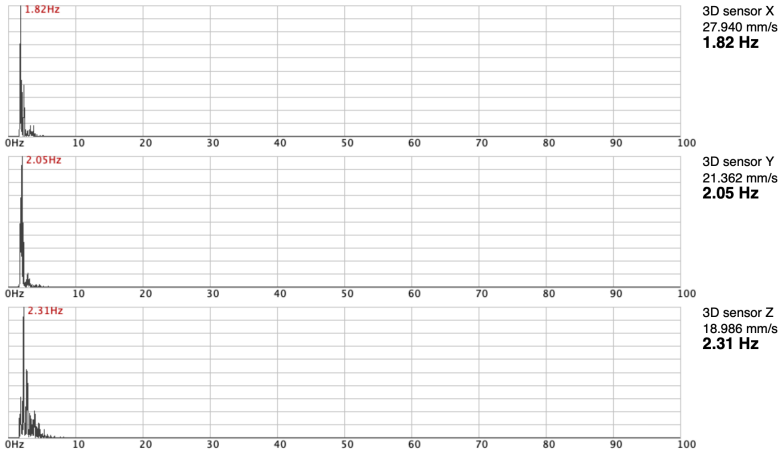

Figure 6: Sample Reconstructed Frequency Distribution

the radius of the Earth is 6371 km. Using the Haversine formula,

$$\phi_1 = latitude_{position} \times \frac{\pi}{180}, \phi_2 = latitude_{epicenter} \times \frac{\pi}{180}$$

$$\delta_1 = longitude_{position} \times \frac{\pi}{180}, \delta_2 = longitude_{epicenter} \times \frac{\pi}{180}$$

Then, with the positions in radians, the distance can be determined.

$$d = 2R \times sin^{-1}\left(\sqrt{sin^2\frac{(\phi_2 - \phi_1)}{2} + cos(\phi_1) \times cos(\phi_2) \times sin^2\frac{(\delta_2 - \delta_1)}{2}}\right)$$

For the case of geographic location (-38.0481, 145.3600) or (-0.6641 rad, 2.5396 rad), and epicenter (-37.1362, 145.51147) or (-0.64815 rad, 2.5370 rad), the distance can be calculated as follows:

$$d = 2(6371km) \times sin^{-1}\sqrt{sin^2\frac{(-0.6641 + 0.64815)}{2} + cos(-0.6641)cos(-0.64815)sin^2\frac{(2.5396 - 2.5370)}{2}}$$

$$d = 2(6371km) \times sin^{-1}\sqrt{0.0000000198886}$$

$$d = 2(6371km) \times sin^{-1}0.00014103$$

$$d = 2(6371km) \times 0.00808025$$

$$d = 102.96km$$

This represents only the horizontal change. The vertical change, through amplitude, is minimal and does not increase the distance by an order larger than 0.01. Here, each distance corresponds to frequencies in all three dimensions. This equation was applied to all points on the dataset, providing a direction magnitude between points.

Correlations between Frequency and Distance

While exploring earthquake frequencies, there were two core findings that contributed to the investigation. First, there was a definitive relationship between distance and the frequency that a building experiences. Earthquake frequencies, from an epicenter, decay as a function of distance. By converting seismic readings from the time to frequency domains at varying points, an exponential model can be based by comparing distances and the peak frequency at that position.

Second, frequencies exist in multiple directions, and each of these directions provide different insights into the growth or decay of a certain frequency. Within seismic analysis, the Horizontal-to-Vertical Spectral Ratio (HVSR) is a standard to combines the three frequencies as a ratio of

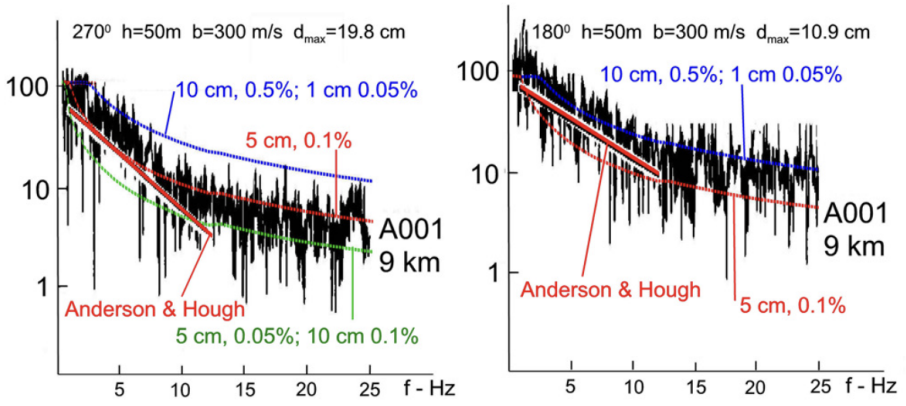

Figure 7: Relationship between Earthquake Frequency and Direction on a Plane (Gičev and Trifunac, 2022)

squares. With three frequencies, this effectively represents the horizontal and vertical movement.

$$HVSR = \frac{x^2_{frequency} + y^2_{frequency}}{z^2_{frequency}}$$

This ratio, commonly used to estimate the resonant frequency of sedimentary layers, effectively demonstrates the Fourier amplitude spectra of the horizontal and the vertical component of microtremors (Mucciarelli, 2004). Using these two findings, earthquake frequencies—when modelled as a function of distance—should provide a negative exponential correlation. In order to determine this graph, the direction magnitudes were plotted against the ratio.

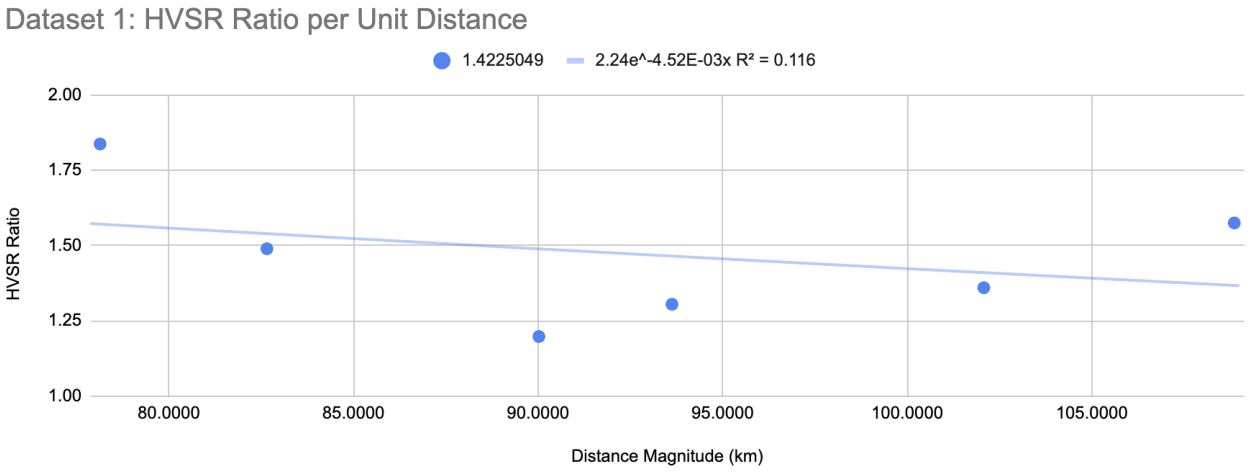

Figure 8: Plot of HVSR against Distance Magnitudes

With an R^2 value of 0.116, there is no clear relationship between the ratio and the distance from the epicenter. This left me confused, questioning whether there was a relationship at all. In an attempt to find a correlation, I switched from the HVSR ratio to the magnitude in order to investigate if there was a different relationship.

$$Frequency_{Magnitude} = \sqrt{Frequency_x^2 + Frequency_y^2 + Frequency_z^2}$$

Nonetheless, with an R^2 value of 0.26, I achieved similar results: no relationship.

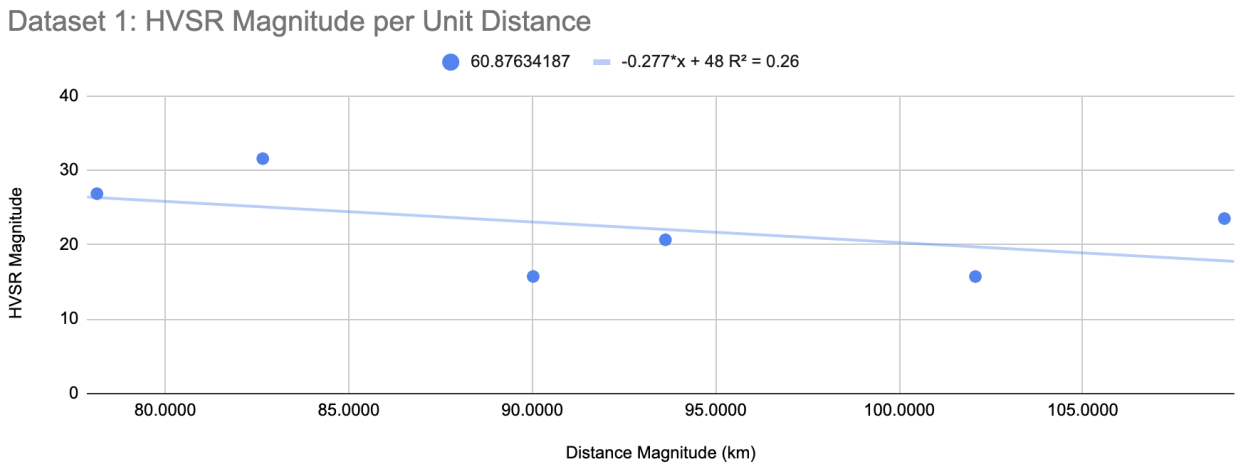

Figure 9: Plot of Frequency Ratio against Distance Magnitudes

This posed a moment of reflection where a correlation involved a deep interplay between a variety of factors. After trying an array of new methods and completing more research into these factors, I encountered a new equation for movement:

$$Movement = \frac{(x_{frequency}^2 + y_{frequency}^2) \times \Delta mm}{(z_{frequency}^2) \times \Delta s}$$

The rate, more specifically particle velocity in mm/s, was a secondary indicator that worked in complement to the frequency distribution. Therefore, movement was calculated as follows:

$$Movement = \frac{(x_{frequency}^2 + y_{frequency}^2) \times Rate}{(z_{frequency}^2)}$$

$$Movement = HVSR \times Rate$$

For example, suppose the rate of an earthquake was $9.750mm/s$ and the three dimensional frequencies of $\begin{smallmatrix} x \\ y \\ z \end{smallmatrix}$ were $\begin{smallmatrix} 35.35 \\ 35.08 \\ 35.01 \end{smallmatrix}$ Hz. The movement of the earthquake at this point is $HVSR \times Rate = 13.869mm/s$. For all datasets, this relationship was applied and graphed accordingly, producing a very strong correlation.

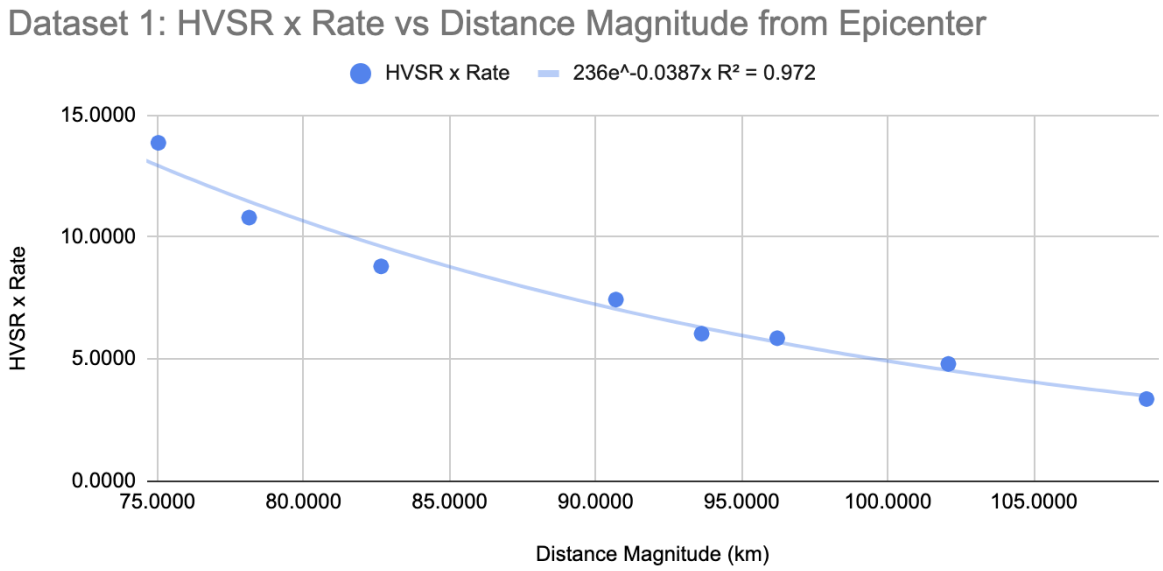

Figure 10: HVSR x Rate vs Distance from Epicenter in Dataset 1

This graph is modeled by the approximate equation: $f(x) = 236e^{-0.039x}$, with correlation of $R^2 = 0.972$. This relationship is quite strong, which prompted me to explore the universality of the relationship. Through the Waves Analysis Software, I explored another earthquake: a magnitude 4.7 earthquake only a few months prior, in November 2022 in Greece, destroying buildings and architecture. Upon applying the same data analysis, the following graph was produced.

This equation, with a significantly higher R^2 value of 0.997, highlights the strong correlation that exists between the distance from the epicenter and its movement. From this relationship, and

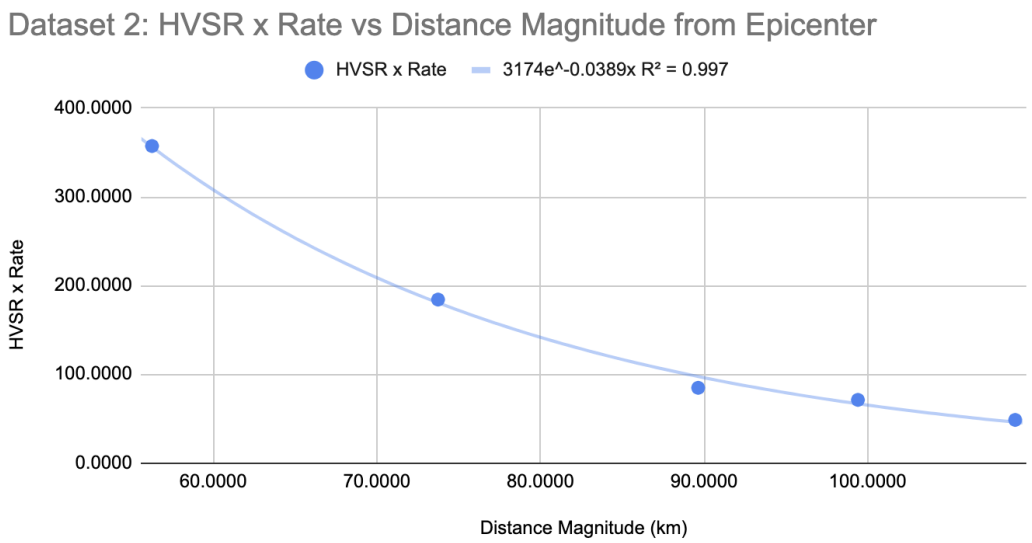

Figure 11: HVSR x Rate vs Distance from Epicenter in Dataset 2

the equation $f(t) = 3174e^{-0.039}$, an equation for the decay with constant C can be simplified:

$$decay = C \times e^{-0.039\,\vec{d}}$$

It was most surprising to see the exponential nature of decay. It was expected to have a logarithmic decay that maintained high frequencies that rapidly decreased at larger distances. As demonstrated in Figure 7, where frequency is on the X axis, frequencies begin to plateau at lower distances. Despite there being a similar graph shape, the axis of Figures 10 and 11 are as a function of distance. Here, the frequencies begin to plateau at higher distances. This, however, brings light to the role of *rate* as a variable and its relationship to frequency decay.

Equation for Decay

For the value of C, an interesting pattern arises between the coefficients of both datasets.

For the first dataset, the equation is $f(t) = 236e^{-0.039t}$ with a magnitude of 8.6 and rate of

$7.969\frac{mm}{s}$. The first dataset has the equation $f(t) = 3174e^{-0.039t}$ with a magnitude of 4.7 and rate of $96.092\frac{mm}{s}$. The coefficients on the exponential functions, through experimentation, were discovered to be as follows:

$$decay = C \times e^{-0.039\,\vec{d}}$$

$$C = e \times rate^{ln(magnitude)}$$

For each coefficient, the quotient between the $rate^{ln(magnitude)}$ and the coefficient was consistently approximately 2.71, which highlights the presence of Euler's number in the real world—natural disasters, specifically. Hence, the equation for the decay of frequencies, where $f(t)$ represents the $HVSR \times Rate$, is as follows:

$$f(d) = e \times Rate^{ln(magnitude)} \times e^{-0.039|\vec{d}|}$$

$$HVSR \times Rate = e \times Rate^{ln(magnitude)} \times e^{-0.039|\vec{d}|}$$

$$HVSR \times Rate = Rate^{ln(magnitude)} \times e^{1-0.039|\vec{d}|}$$

Therefore, a brand new equation for the HVSR as a function of distance can be derived:

$$HVSR = Rate^{ln(magnitude)-1} \times e^{1-0.039|\vec{d}|}$$

To verify the equation, consider an 6.0 magnitude earthquake in Australia in 2021 with a rate at the epicenter at $160.41\frac{mm}{s}$. A certain point, existing $73.3km$ from the epicenter, follows the waveform in Figure 12:

Then, by applying the Discrete Fourier Transform and creating the frequency distribution:

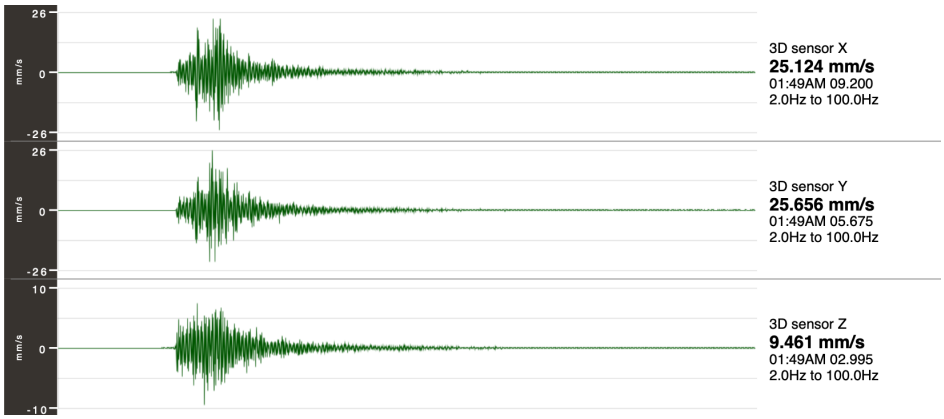

Figure 12: Sample Testing Waveform per Unit Time

Figure 13: Sample Testing Waveform per Unit Frequency

Here, the HVSR can be calculated as:

$$HVSR = \frac{x^2_{frequency} + y^2_{frequency}}{z^2_{frequency}}$$

$$HVSR = \frac{(5.10)^2 + (2.49)^2}{(1.93)^2}$$

$$HVSR = 8.65 \approx 8.7$$

Given the formula, the equation can be applied to verify the rate:

$$HVSR = Rate^{ln(magnitude)-1} \times e^{1-0.039|\vec{d}|}$$

$$HVSR = 160.41^{ln(6.0)-1} \times e^{1-0.039|73.3km|}$$

$$HVSR = 55.7202 \times 0.1555108$$

$$HVSR = 8.67 \approx 8.7$$

This equation verifies the universality of the equation, as the HVSR can be effectively verified for three earthquakes: (1) 8.6 Magnitude Earthquake in Indian Ocean (2) 4.7 Magnitude Earthquake in Greece (3) 6.3 Magnitude Earthquake in Australia. Given the accuracy and precision of the data, this information can help revisit the initial earthquake of inspiration.

Due to the three dimensional nature of earthquakes, a single frequency cannot be isolated for resistance. Instead, by using the ratio and historical extrapolations, it is projected that buildings that can resist HVSR frequency ratios up to 105.95 will be most effective. This finding can serve to significantly speed up mechanisms of testing and consider the destructive three-dimensional frequencies that cause the most damage.

Conclusion

Building design is an expensive and lengthy process, one that can take significant amounts of testing and optimization before put into production. In economically disadvantaged areas, the same privilege of extensive testing may not be possible.

This investigation sought to explore the relationship between distance from the epicenter and the frequencies of an earthquake, in order to optimize the construction and testing of earthquake-

resistant buildings in the most cost-efficient manner. The initial postulation, that the movement of a building corresponds to the movement of the earthquake at that point, was a guiding force in the investigation.

By deriving a new equation for the Discrete Fourier Transform in the context of a seismic wave, in complement to the algorithm that plotted particle velocities as a function of frequency, direct correlations could be discovered between the movement, defined as $HVSR \times Rate$, and the distance from the epicenter. In doing so, a brand new equation for HVSR was derived as follows:

$$HVSR = Rate^{ln(magnitude)-1} \times e^{1-0.039|\vec{d}|}$$

This equation was of great significance as it proposed a more comprehensive way to test and optimize buildings to withstand siesmic events. The damaging nature of earthquakes, that is often overlooked, is the three-dimensional nature of movements. As a result, the new equation for HVSR estimates what frequencies or styles of testing can be employed.

Next Steps

In the future, I hope to identify the role of other variable factors in the derived equation. For example, recent studies have indicated how the rating of soil—on a scale from "A" to "F"—may influence design choices of earthquake-resistant architecture (Nolan, 2022). Furthermore, I hope to further apply these findings in a scientific setting and determine optimal building shapes, that explores the most earthquake-resistant design with the lowest cost of production. This may be of particular interest with the recent Syria-Turkey earthquakes, where poor testing in infrastructure and buildings resulted in significant damages across the nation (Bateman and Gozzi, 2023).

Nonetheless, this exploration has allowed me to explore the relationship between the most fundamental pieces geological information, and apply them to mathematically optimize earthquake-

resistant buildings using the Fourier Transform. The investigation, while demonstrating the natural beauty of Euler's number e, also enabled a more thoughtful exploration of how frequency analysis can rethink building design, helping organizations avoid investments in repetitively rebuilding infrastructure and support victims of natural disasters in the most meaningful ways possible.

Bibliography

Aldeen, S. (2020). *Digital Convolution with Digital Signal Processing (DSP).* Retrieved February 11, 2023, from https://papers.ssrn.com/sol3/papers.cfm?abstract=3647517.

Bateman, B. T. and Gozzi, L. (2023). *Turkey issues 113 arrest warrants connected to building construction.* Retrieved February 12, 2023, from https://www.bbc.com/news/world-middle-east-64615349.

Gičev, V. and Trifunac, M. D. (2022). *High-frequency decay of Fourier spectra of strong motion acceleration and nonlinear site response.* Retrieved February 11, 2023, from https://onlinelibrary.wiley.com/doi/full/10.1002/eer2.28.

Manoa, H. (2007). *Compare-Contrast-Connect: Seismic Waves and Determining Earth's Structure.* Retrieved February 12, 2023, from https://manoa.hawaii.edu/exploringourfluidearth/physical/ocean-floor/layers-earth/compare-contrast-connect-seismic-waves-and-determining-earth-s-structure.

Mucciarelli, M. (2004). *The HVSR technique from microtremor to strong motion: empirical and statistical considerations.* Retrieved February 11, 2023, from https://www.iitk.ac.in/nicee/wcee/article/13_45.pdf.

Nolan, J. (2022). *The Effects of Soil Type on Earthquake Damage.* Retrieved February 11, 2023, from https://www1.wsrb.com/blog/the-effects-of-soil-type-on-earthquake-damage.

Pekar, D. (2020). *Engineering Math: Fourier Analysis and Earthquake Engineering.* Retrieved February 11, 2023, from https://seismic.skule.ca/academy.

Shigefuji, M., Takai, N., and Bijukchhen, S. (2022). *Strong ground motion data of the 2015 Gorkha Nepal earthquake sequence in the Kathmandu Valley.* Retrieved February 11, 2023, from https://www.nature.com/articles/s41597-022-01634-6.